Applied Microbiology and Biotechnology (2021) 105:1421–1434
https://doi.org/10.1007/s00253-020-11050-8

BIOTECHNOLOGICAL PRODUCTS AND PROCESS ENGINEERING

High cell density perfusion process for high yield of influenza A virus production using MDCK suspension cells

Yixiao Wu[1,2] · Thomas Bissinger[2] · Yvonne Genzel[2] · Xuping Liu[1,3] · Udo Reichl[1,4] · Wen-Song Tan[1]

Received: 30 June 2020 / Revised: 1 December 2020 / Accepted: 9 December 2020 / Published online: 30 January 2021

Abstract

Similar to the recent COVID-19 pandemic, influenza A virus poses a constant threat to the global community. For the treatment of flu disease, both antivirals and vaccines are available with vaccines the most effective and safest approach. In order to overcome limitations in egg-based vaccine manufacturing, cell culture–based processes have been established. While this production method avoids egg-associated risks in face of pandemics, process intensification using animal suspension cells in high cell density perfusion cultures should allow to further increase manufacturing capacities worldwide. In this work, we demonstrate the development of a perfusion process using Madin-Darby canine kidney (MDCK) suspension cells for influenza A (H1N1) virus production from scale-down shake flask cultivations to laboratory scale stirred tank bioreactors. Shake flask cultivations using semi-perfusion mode enabled high-yield virus harvests (4.25 $\log_{10}$(HAU/100 μL)) from MDCK cells grown up to 41×10^6 cells/mL. Scale-up to bioreactors with an alternating tangential flow (ATF) perfusion system required optimization of pH control and implementation of a temperature shift during the infection phase. Use of a capacitance probe for on-line perfusion control allowed to minimize medium consumption. This contributed to a better process control and a more economical performance while maintaining a maximum virus titer of 4.37 $\log_{10}$(HAU/100 μL) and an infectious virus titer of 1.83×10^{10} virions/mL. Overall, this study clearly demonstrates recent advances in cell culture–based perfusion processes for next-generation high-yield influenza vaccine manufacturing for pandemic preparedness.

Key points

- *First MDCK suspension cell–based perfusion process for IAV produciton was established.*
- *"Cell density effect" was overcome and process was intensified by reduction of medium use and automated process control.*
- *The process achieved cell density over 40 × 10^6 cells/mL and virus yield over 4.37 $\log_{10}$(HAU/100 μL).*

Keywords MDCK cells · Influenza A virus · ATF-based perfusion · Process optimization · Lab-scale bioreactors

Introduction

The current pandemic of coronavirus disease (COVID-19) has spread to over 200 countries and territories and poses a severe public health emergency (Hoffmann et al. 2020). Similarly, the rise of influenza A virus (IAV) epidemics in both northern and southern hemisphere poses an unpredictable threat to the human health and a severe challenge for the global economy (Fauci 2006; Yamayoshi and Kawaoka 2019). Compared to the coronavirus pandemic with no vaccines available at time of emergency, for influenza virus, vaccination that remains the safest and most effective approach to prevent IAV infection and spread is available (Lambert and Fauci 2010). Concerning millions of people at risk, fast and high-yield production of vaccines should be the focus of the pharmaceutical industry to prevent the next emerging virus threat.

✉ Xuping Liu
xupingliu@ecust.edu.cn

[1] State Key Laboratory of Bioreactor Engineering, East China University of Science and Technology, 130 Meilong Road, Shanghai 200237, China

[2] Bioprocess Engineering Group, Max Planck Institute for Dynamics of Complex Technical Systems, Sandtorstrasse 1, 39106 Magdeburg, Germany

[3] Shanghai BioEngine Sci-Tech Co., Ltd, 781 Cailun Road, Shanghai 201203, China

[4] Chair of Bioprocess Engineering, Otto-von-Guericke University Magdeburg, Universitaetsplatz 2, 39106 Magdeburg, Germany

With the current manufacturing capacity of the traditional egg-based production platform, about 1.5 billion seasonal influenza doses were estimated to be produced in 2015 for the entire world population (McLean et al. 2016). However, in the event of an IAV pandemic emergency, even this might be insufficient to meet the global demand in a short time period due to the lack of egg supply and manufacturing facilities. In addition, process yields might be too low, i.e., for avian influenza virus strains that do not replicate to high titers in eggs. Furthermore, vaccines might be less effective due to antigenic changes after virus propagation in eggs. Today, animal cell culture–based production technologies have become a viable alternative to embryonated chicken eggs for inactivated influenza vaccines. Various cell lines, including HEK293, AGE1.CR, PER.C6, Vero, and MDCK, have shown their potential as the substrate for IAV propagation to increase overall manufacturing capacity and efficiency (Genzel and Reichl 2009; Hu et al. 2011; Kistner et al. 1999). Among these, MDCK cells show a superior productivity and applicability, and various MDCK cell–derived influenza vaccines regarding Flucelvax®/Optaflu® (Seqirus/Novartis) and SKYCellflu® (SK chemicals) have already been certified (Genzel and Reichl 2009; Sun et al. 2011). In view of the relatively complicated cultivation of adherent MDCK cells, single MDCK suspension cells that grow with short doubling time in serum-free medium and that have a high virus productivity have been developed, thanks to successful directed medium development (Bissinger et al. 2019; Huang et al. 2015; Xie et al. 2019).

Cell culture–based processes for virus production comprise two phases, the cell amplification phase followed by the virus propagation phase. To achieve high virus yields, critical factors such as the viable cell concentration, the preparation of seed virus with an optimized multiplicity of infection (MOI), and harvest timing should be evaluated (Tapia et al. 2016). Considering this, intensified and high cell density (HCD) processes with concentrations above 20×10^6 cells/mL are applied by increasing the cell concentration either by fed-batch or perfusion strategies. As applied for antibody production processes, perfusion cultures allow to increase the productivity, reduce process costs, and minimize the impact of undesired byproducts as well as osmolality (Konstantinov et al. 2006; Rodriguez et al. 2010; Sandberg et al. 2006; Walther et al. 2015). Most of the equipment required is even available for single-use operation. Furthermore, it is also needed for a fast response in case of an influenza pandemic.

Cell retention devices play an important part in the perfusion culture. The alternating tangential flow (ATF) filtration has emerged as one of most commonly used strategies for process intensification for virus production at laboratory scale. A wide range of cell lines targeting very high cell concentrations (up to 180×10^6 cells/mL) have been evaluated with this technology for the production of various virus types, such as IAV, Modified Vaccina Ankara (MVA) virus, yellow fever virus, and Zika virus. (Bissinger et al. 2019; Coronel et al. 2019; Granicher et al. 2019; Nikolay et al. 2018; Vazquez-Ramirez et al. 2019). In ATF-based perfusion cultures with continuous feeding of fresh medium and withdrawal of spent medium, proper control strategies need to be selected to ensure continuous nutrient supply for the cultivated cells. Furthermore, in the infection phase of HCD processes, optimal operating conditions have to be selected for virus propagation to overcome the so-called "cell density effect"—a reduction of cell-specific virus yield (CSVY) (Henry et al. 2004; Maranga et al. 2003). For process monitoring and control, the use of capacitance probes proved to be a good strategy for recombinant protein and viral vaccine production (Ansorge et al. 2007; Carvell and Dowd 2006; Emma and Kamen 2013; Kiss and Németh 2016). With the aim of increasing virus productivity, process conditions have been optimized at HCD for IAV virus production processes using various cell lines (Coronel et al. 2019; Genzel et al. 2014; Nikolay et al. 2018; Vazquez-Ramirez et al. 2019). Nevertheless, obtained CSVYs were still rather low, and did not contribute to the high virus titers achieved in these processes. However, a MDCK suspension cell line cultivated in chemically defined medium (CDM) and that showed superior cell growth performance and high CSVY compared to other MDCK cells (Bissinger et al., submitted) suggested the great potential for further process intensification and high-yield production.

In this study, we present an optimized ATF-based perfusion process for IAV production using this newly established and highly productive MDCK suspension cell line grown in CDM. First, shake flask (SF) experiments were performed as a scale-down model to investigate the cell growth and virus production at HCD. In a next step, the process was transferred to laboratory scale bioreactors and optimized regarding pH control and temperature regime to increase virus productivity. Finally, a high-yield perfusion process with a low cell-specific perfusion rate (CSPR) and the use of a capacitance probe for perfusion rate control was evaluated. Results clearly demonstrate that the established perfusion process is well suited for fast and efficient influenza vaccine manufacturing in animal cells, particularly in the case of pandemic emergency.

Materials and methods

Cell line and cell culture

The MDCK suspension cell line was obtained by adapting a formerly established suspension cell line (originally from adherent cells (NBL-2, ATCC CCL-34) that grow in serum-free medium (Xeno-SFM; Bioengine, China)) to growth in a newly developed CDM (Xeno-CDM1; Bioengine, China) in four passages (Huang et al. 2015). MDCK cells were cultivated in

non-baffled polycarbonate Erlenmeyer shake flasks (Corning®, Corning, USA) in an orbital shaking incubator (Infors HT, Switzerland) at 37 °C, 5% CO_2 atmosphere, with a shaking frequency of 100 rpm. For further experiments in bioreactors, this new MDCK cell line was further adapted over two passages to grow in an updated version of Xeno-CDM1 with the superior buffer capacity, here named Xeno-CDM2.

Cell concentration, viability, and diameter were measured by a cell counter with trypan blue staining (Vi-CELL XR, Beckman Coulter, USA). Glucose, glutamine, lactate, and ammonium were determined by a Bioprofile 100 plus (Nova medical, USA) with external standards. Culture osmolality was measured by an osmometer (VAPRO® 5520, Wescor, USA). Amino acid concentration was determined using an Acquity H-Class UPLC instrument (Waters, USA).

Virus infection

The virus strain influenza A/PR/8/34 H1N1 (Robert Koch Institute, Germany, Amp. 3138) (here IAV for short) derived from adherent MDCK cells (ECACC, Public Health, UK) was used for adaptation to the MDCK suspension cell line in Xeno-CDM1 over five passages with a MOI of 10^{-5}. After adaptation, the infectious titer of the final seed virus was 1.8×10^9 virions/mL.

Trypsin (Gibco, USA, #27250-018, prepared in PBS to 5000 U/mL) was supplemented to the cultivation as well as to the perfusion medium for the complete infection phase to a final trypsin activity of 20 U/mL. All the infections in shake flasks were performed with the replacement of the spent medium at the time of infection (TOI). All the infections in bioreactors were conducted after partial medium replacement by increasing the pump rate to 150 mL/h for 2 h. Diluted IAV seed virus was added with a MOI of 0.001.

Semi-perfusion cultures in shake flasks

Semi-perfusion studies were carried out with a CSPR-based strategy to achieve high cell densities in shake flasks ($n = 2$). In order to mimic the perfusion process in bioreactors, the medium volume exchanged (V_E) in SFs followed Eq. (1) derived from continuous perfusion process strategies:

$$V_E = \frac{(e^{\mu \Delta t} - 1)\, x_i}{\mu}\, V_w\, \mathrm{CSPR} \quad (1)$$

Δt	time interval between two sampling points (h)
μ	cell-specific growth rate (1/h)
x_i	viable cell concentration (cells/mL)
V_w	working volume (mL)
CSPR	cell-specific perfusion rate (pL/cell/h)

MDCK cells were cultivated in baffled SFs and medium exchange was started at 48 h. For each perfusion step, the medium volume to be exchanged was calculated based on the increasing cell concentration. Later, the time interval for the medium exchange was shortened and the exchange volume was fixed to 60–70% V_w to achieve a constant CSPR. At each perfusion step, the calculated volume (or 60–70% V_w) of the culture was centrifuged (300×*g*, 10 min) and the supernatant was discarded. Subsequently, the cell pellet was resuspended with fresh and pre-warmed medium.

Perfusion cultures in bioreactors

For the perfusion processes (ATF1-ATF5 run), an ATF2 system with the C24U-v2 controller (Repligen, USA) was used. Therefore, a 1 L DASGIP® bioreactor (Eppendorf, Germany) (500 mL V_w) was connected to an ATF unit (hollow-fiber module, 0.2 μm pore size, 470 cm^2, Spectrum Labs, USA). Aeration was realized by a micro- (ATF1) or macrosparger (ATF2–5) with air-O_2 mixture to a dissolved oxygen (DO) set point of 40%. The pH value was controlled by sparging CO_2 and 7.5% $NaHCO_3$ addition (for the ATF1 run 1 M NaOH was used). pH values of 7.00 or 7.15 were used for the cell growth phase and 7.20 for the virus infection phase. Cells were grown and perfused in Xeno-CDM1 (ATF1) or Xeno-CDM2 (ATF2–5). After 48–65-h batch cultivation, the perfusion unit was started by using the diaphragm pump of the ATF system. The flow rate in the hollow fiber was set at 0.7–1.0 L/min. Meanwhile, feed and harvest pumps were started. While the temperature in the cell growth phase was set to 37 °C, it was decreased to 33 °C at TOI starting with the ATF3 run; afterwards this strategy was applied to all subsequent bioreactor runs.

In the ATF5 run, a capacitance probe (Incyte, Hamilton, Switzerland) was used for on-line monitoring of the viable cell concentration for the perfusion rate control. The capacitance probe was connected to an Arc View controller 265 (Hamilton, Switzerland) for recording and plotting permittivity measurements. The on-line measured permittivity can be correlated to the viable cell concentration (VCC). Based on a linear regression, the slope between the permittivity signal and VCC was determined as "cell factor" to correct the controller. For the perfusion rate control, the output signal was transmitted through a ComBox (Hamilton, Switzerland) to the DASware® control software (Eppendorf, Germany). By converting the output signal to the perfusion rate, the software controlled the peristaltic pumps to adjust the medium feed. Based on the constant measurement of the vessel mass, the feed pump rate was synchronized to the permeate pump rate by the DASware® control software to preserve a constant V_w.

With a constant CSPR of 60 or 40 pL/cell/day, the perfusion rate (Q, mL/h) was calculated according to Eq. (2) and

controlled or adjusted manually in all runs after the perfusion was started.

$$Q = x_i \, e^{\mu \Delta t} \, V_w \, \mathrm{CSPR} \tag{2}$$

Virus quantification

The total amount of IAV particles was determined with the hemagglutination assay with a standard deviation of 0.081 $\log_{10}$(HAU/100 μL) (Kalbfuss et al. 2008). To quantify the concentrations of infectious virus particles, a $TCID_{50}$ assay was used with a dilution error equal to ± 0.3 $\log_{10}$(infectious virions/mL) as described previously by Genzel and Reichl (Genzel and Reichl 2007). Due to the multiple harvesting of virus particles during the medium replacement for the semi-perfusion and the continuous removal of virus particles from the bioreactor to the permeate through the ATF membrane for the bioreactor runs, an accumulated HA titer (HA_{acc}, $\log_{10}$(HAU/100 μL)) and $TCID_{50}$ titer ($TCID_{50,acc}$, virions/mL) were determined (Eqs. (3) and (4)). These values represent the theoretical virus titers in the cultivation vessel without any transfer of viruses to the permeate.

$$\mathrm{HA_{acc}} = \log_{10} \frac{\sum\left(10^{\mathrm{HA_v}} \times V_w + 10^{\mathrm{HA_h}} \times V_h\right)}{V_w} \tag{3}$$

$$\mathrm{TCID_{50,\ acc}} = \frac{\sum\left(\mathrm{TCID_{50,BR}} \times V_w + \mathrm{TCID_{50,h}} \times V_h\right)}{V_w} \tag{4}$$

HA_v HA titer in the SF or the bioreactor vessel, $\log_{10}$(HAU/100 μL);

HA_h HA titer in SF experiments or average HA titer in bioreactor runs in each harvest step, $\log_{10}$(HAU/100 μL);

$TCID_{50,BR}$ $TCID_{50}$ titer in the SF or the bioreactor vessel, virions/mL.

$TCID_{50,h}$$TCID_{50}$ titer in SF experiments or average $TCID_{50}$ titer in bioreactor runs in each harvest step, virions/mL.

The total number of virus particles per volume (C_{tot}, virions/mL) was calculated by multiplying the virus titer and erythrocyte concentration as given by Eq. (5). The cell-specific virus yield (CSVY, virions/cell), space time virus yield (STVY, virions/L/day), and volumetric virus productivity (P_v, virions/L/day) based on HA titer were calculated as given by Eqs. (6), (7), and (8). Based on the standard deviation of the HA assay, the error of C_{tot}, CSVY, STVY, and P_v equals to 20.5% for the upper value and 17.0% for the lower value.

$$C_{tot} = 2 \times 10^7 \times 10^{\mathrm{HA_{acc}}} \tag{5}$$

$$\mathrm{CSVY} = \frac{C_{tot,max}}{X_{v,max}} \tag{6}$$

$$\mathrm{STVY} = \frac{C_{tot,max}}{t_h} \tag{7}$$

$$P_v = \frac{C_{tot,max} \times V_w}{V_h \times t_h} \tag{8}$$

$X_{v,max}$ maximum viable cell concentration at the time point of highest virus titer, cells/mL.

$C_{tot,max}$ maximum total virus concentration, virions/mL.

t_h total time from cell culture start until potential harvest time point, day.

V_h total medium volume spent from cell culture start until potential harvest time point, mL.

Results

Influenza A virus production at HCD in shake flasks

In a study performed in parallel, a highly efficient batch process for H1N1 influenza A virus production with the same MDCK suspension cell line and cultivation medium (XenoCDM1) was establisehd (Bissinger et al., submitted). Viable cell concentrations up to 7×10^6 cells/mL in the infection phase resulted in high virus titers of up to 3.60 $\log_{10}$(HAU/100 μL) (data not shown). As a starting point to investigate the potential of this MDCK suspension cell line for further process intensification, HCD cultivations in SFs were conducted.

Therefore, a CSPR-based strategy for "perfusion rate" control was implemented for the cultivation of MDCK suspension cells in semi-perfusion mode. A CSPR of 60 pL/cell/day was applied based on previous investigations (Bissinger et al. 2019). To calculate the volume of medium to be exchanged with each harvest step, a constant specific growth rate of 0.027 h^{-1} was assumed. With this feeding strategy, cell concentrations up to 40×10^6 cells/mL were achieved over 5 days despite a reduction of the actual growth rate from 0.037 to 0.016 h^{-1} before infection (Fig. 1a). Cells continued to grow after seed virus addition in SFs and a maximum cell concentration (47×10^6 cells/mL) was reached at 18 h post infection (hpi) with the onset of virus accumulation. The virus titer started to decrease after reaching 4 $\log_{10}$(HAU/100 μL) due to the virus revomal at each harvest step (Fig. 1c). The HA_{acc} was calculated to estimate the overall virus yield to compare the batch, semi-perfusion, and perfusion processes. As expected, virus titers increased rapidly and reached a plateau at 4.25 $\log_{10}$(HAU/100 μL) at 40 hpi, which corresponds to a total virus concentration of 3.6×10^{11} virions/mL (Fig. 1d). This

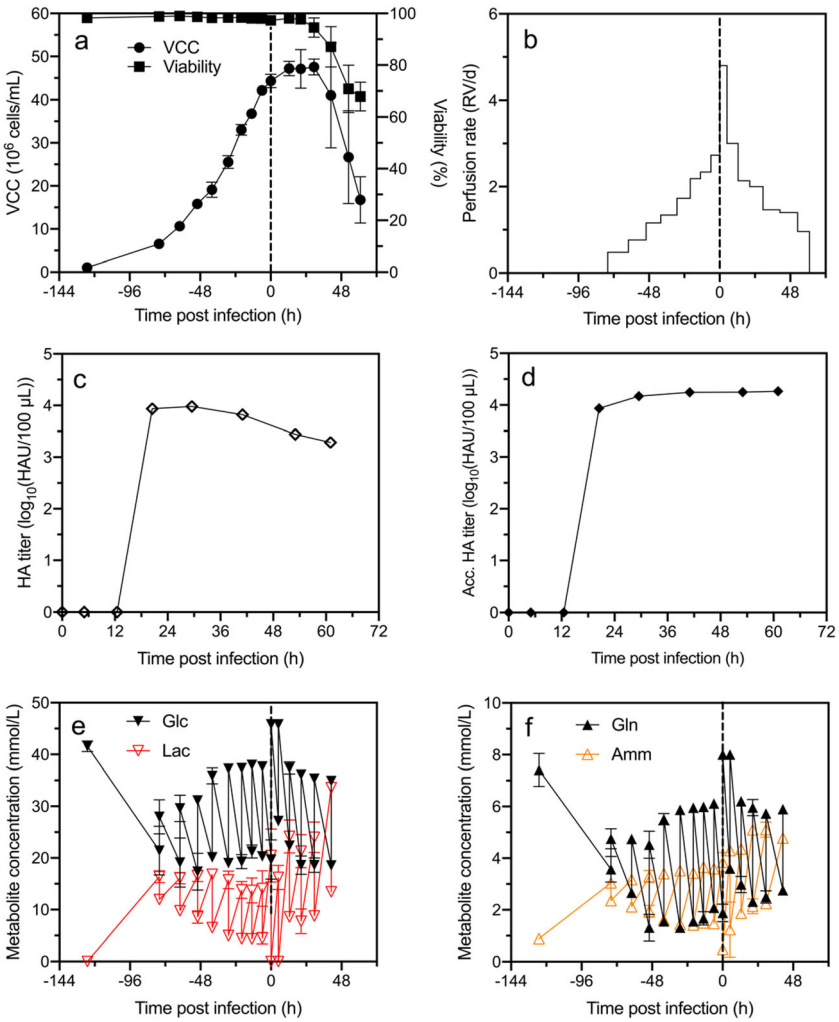

Fig. 1 MDCK suspension cell cultivation in shake flasks for IAV production at high cell density. (a) Viable cell concentration and viability, (b) perfusion rate, (c) HA titer in the culture vessel, (d) HA_{acc} titer of multiple harvests, (e) glucose (Glc) and lactate (Lac) concentration, and (f) glutamine (Gln) and ammonium (Amm) concentration. Medium exchange was initiated 48 h after inoculation. Vertical dashed lines indicate time of infection. The error bars represent the standard deviation of duplicate experiments

represents a 4.5-fold increase compared to the batch cultivation (Table 3). Due to the manual addition of medium in semi-perfusion mode (based on the CSPR-based feeding strategy), a stepped RV/day profile was obtained (Fig. 1b). The complete media replacement at TOI resulted in a peak of the "perfusion rate" of 4.8 RV/day.

The multiple medium exchange steps resulted in a saw-toothed profile of the concentrations of the main extracellular metabolites. Overall, the measured metabolite concentrations (Fig. 1e and f) and the specific consumption rates (data not shown) were stable, despite increasing cell concentrations, indicating that the cells were in a "similar" physiological states (Konstantinov et al. 2006). The measured concentrations of extracellular glucose and lactate did not indicate any limitations over the whole cultivation; the minimum glucose concentration was above 10 mM, while the maximum lactate concentration did not exceed 35 mM. Accordingly, the decrease in the specific growth rate seemed not to be caused by a limitation of main substrates or toxic by-product accumulation, but by some other critical medium components that were not measured. After infection, a notable increase in lactate and ammonium production was observed, which could have a potential negative impact on the virus yield.

In summary, the growth to concentrations up to 47×10^6 cells/mL with a maximum virus titer of 4.25 log_{10}(HAU/100 µL) was achieved in SFs in semi-perfusion mode for HCD cultivation in Xeno-CDM1. Based on this result, the establishment of a fully controlled perfusion processes in a bioreactor seemed promising.

Process optimization in bioreactors at HCD

As a starting point, the first bioreactor run (ATF1) was carried out with operating conditions mimicking as closely as possible the perfusion strategy, the target cell concentration for infection, and the infection strategy of SF cultivations. For process optimization, additional cultivations were carried out (ATF2 and ATF3). In particular, the pH control was optimized both for growth and infection phase (ATF2), and temperature during infection phase was lowered (ATF3) (Table 1).

Table 1 Process parameters of bioreactor runs ATF1 to ATF5

Parameter	ATF1	ATF2	ATF3	ATF4	ATF5
pH ± deadband[a]	7.00±0.02 (cell growth) 7.20±0.02 (virus infection)	7.15±0.02 (cell growth) 7.20±0.02 (virus infection)	7.15±0.02 (cell growth) 7.20±0.02 (virus infection)	7.15±0.02 (cell growth) 7.20±0.02 (virus infection)	7.15±0.02 (cell growth) 7.20±0.02 (virus infection)
DO (%)	40	40	40	40	40
Temperature (°C)	37 (cell growth) 37 (virus infection)	37 (cell growth) 37 (virus infection)	37 (cell growth) 33 (virus infection)	37 (cell growth) 33 (virus infection)	37 (cell growth) 33 (virus infection)
Agitation (RPM)	100	100	100	100	100
Aeration	Microsparger	L-Macrosparger	L-Macrosparger	L-Macrosparger	L-Macrosparger
Medium	Xeno-CDM1	Xeno-CDM2	Xeno-CDM2	Xeno-CDM2	Xeno-CDM2
CSPR (pL/cell/day)[b]	60	60	60	40	40 (on-line control)

DO, dissolved oxygen; *CSPR*, cell-specific perfusion rate; *ATF*, alternating tangential flow; *MOI*, multiplicity of infection; *CDM*, chemically defined medium

[a] The values of pH ± deadband, DO%, temperature, agitation, CSPR, and ATF flow rate are the set points of the process

[b] For ATF1-ATF4, the CSPR was controlled manually

In the initial perfusion cultivation (ATF1), the cell concentration reached 41×10^6 cells/mL in the cell growth phase. However, compared to the SF cultivations, a lower specific growth rate and a reduced cell viability (below 90%) were observed (Fig. 2a). Operating the ATF recirculation loop without feeding and harvesting (no perfusion flow) at a low cell concentration (2×10^6 cells/mL), we observed a negative impact on cell growth (data not shown). Initiating the ATF perfusion mode later (48 h to 65 h) improved growth rate and viability. Furthermore, pH control failed with the cell concentration exceeding 35×10^6 cells/mL. Accordingly, during the late cell growth phase and the early infection phase, the pH value dropped to 6.8. Base addition (1 M NaOH) during the infection phase was not an option since this typically leads to massive cell aggregation and a drop in viable cell concentration. Since the lactate level was stable during the perfusion, the pH drop was likely caused by CO_2 accumulation in the culture. Nevertheless, a maximum HA titer of 3.92 $\log_{10}$(HAU/100 µL) (corresponding to 1.7×10^{11} virions/mL) was achieved. The virus titer in the harvest vessel was very low (0.81 $\log_{10}$(HAU/100 µL)) and was therefore neglected (< 1% of HA in the bioreactor). However, a

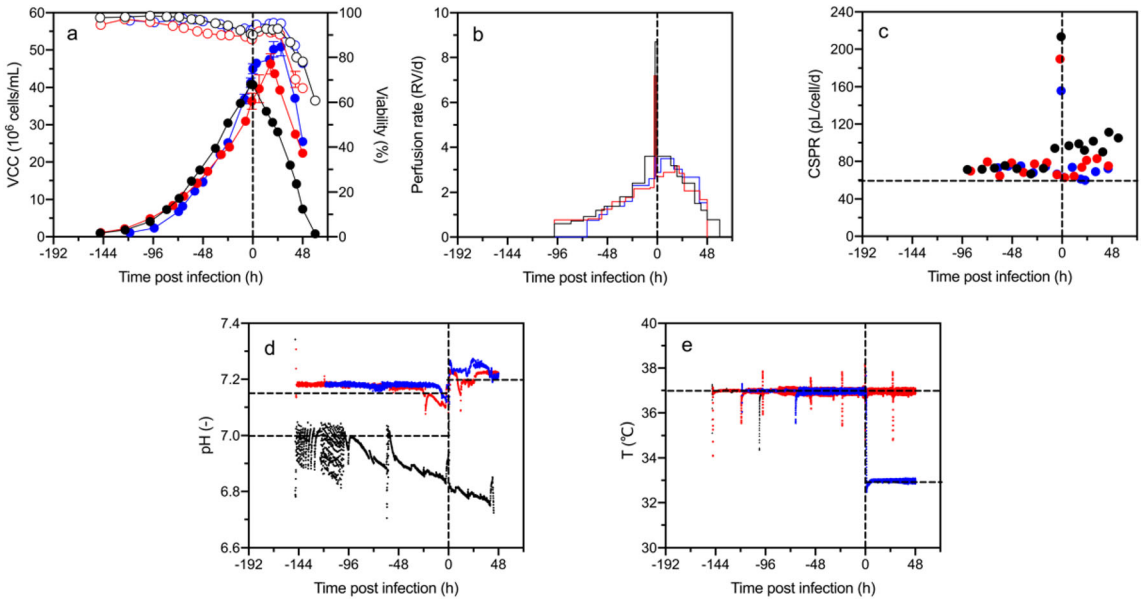

Fig. 2 Process optimization for ATF-based bioreactor perfusion cultures using MDCK suspension cells at high cell density. (a) Viable cell concentration and viability, (b) perfusion rate, (c) cell-specific perfusion rate (CSPR), (d) pH value, and (e) temperature. ATF1 (●), ATF2 (●), ATF3 (●). Perfusion was initiated at 48–65 h after inoculation. Vertical dashed lines indicate time of infection. Horizontal dashed lines indicate set points of process parameters for all runs

reduction of CSVY to 4077 virions/cell at high cell concentration was obtained compared to the batch (Table 3). Despite the initial challenges in operating an ATF-based perfusion process in a bioreactor, the SF scale-down model seemed to be a good tool to evaluate the potential process performance (Table 2). It is clear, however, that there are equally limitations of the scale-down model regarding gas supply, pH, foam control, and ATF performance, to name a few.

As the virus stability and infectivity can be decreased under slightly acidic conditions, the pH in the infection phase should be controlled stably and at proper range (Jia et al. 2016). For a better pH control in the infection phase, various process modifications were tested in scouting experiments and implemented with the ATF2 run. Firstly, instead of a microsparger, a L-macrosparger was used to improve CO_2 stripping and to reduce the risk of foam formation. Still, the macrosparger was able to supply enough oxygen to achieve MDCK cell concentrations of up to 60×10^6 cells/mL with a stable DO level at 40% (data not shown). Furthermore, continuous base addition was tested to stabilize pH at set points. However, both the addition of 1 M NaOH and 0.25 M Na_2CO_3 led to massive cell aggregation and a decrease in the overall viable cell concentration. However, pH control using 7.5% $NaHCO_3$ starting from the time of inoculation was successful for the ATF2 run. Most likely, this was supported by the use of an optimized medium (Xeno-CDM2) with a higher $NaHCO_3$ concentration to improve the medium buffer capacity. To reduce the risk of an unwanted pCO_2 increase, the pH setpoint was increased to 7.15 in the cell growth phase. As a result, the pH value was stable over the whole cell growth phase. During the virus infection phase, the pH was controlled at 7.20 as before. Compared to the virus yield in the ATF1 run, a slightly higher virus titer of 4.12 $\log_{10}$(HAU/100 μL) (2.6×10^{11} virions/mL) and CSVY of 5694 virions/cell were measured in the ATF2 run (Fig. 3b).

The optimization of the pH control resulted in a better process performance and a slight increase in HA_{acc}, but the CSVY was significantly lower compared to the batch process (10,476 virions/cell), which seemed to be a demonstration of a "cell density effect" as described above. As an important process parameter, the temperature may influence the cell behavior and virus replication (Nakamura et al. 2019). Thus, we compared the effect of 37 °C and 33 °C applied in the virus infection phase in HCD cultivations on the cell growth, virus replication, and virus retention in a subsequent run (ATF3). Lower temperature in the ATF3 run suppressed the cell growth in the early infection phase leading to a delay of 10 h for the peak cell concentration compared to the ATF2 run (Fig. 2a). As expected, a delay of virus accumulation under lower temperature condition (ATF3) was also observed, but a HA titer (4.21 $\log_{10}$(HAU/100 μL)) similar to the ATF2 run was measured in the bioreactor (Fig. 3a). Interestingly, a rather high HA titer (45% of the virus concentration in the bioreactor) was found in the harvest vessel in this run, while only very low titers were found in the harvest of the ATF1 and ATF2 runs (Fig. 3c). Thus, virus particles in the harvest were taken into account for the evaluation of overall virus yield (Table 3). With a HA_{acc} of 4.37 $\log_{10}$(HAU/100 μL) (4.7×10^{11} virions/mL), the overall virus yield of the ATF3 run was 1.8-fold higher than the ATF2 run and 3-fold higher than the ATF1 run, respectively. The CSVY increased from 5694 virions/cell (ATF2) to 9229 virions/cell. In addition, the STVY in the ATF3 run was 1.9-fold higher than for the ATF2 run (Table 3). Overall, all these results suggested a successful implementation of a temperature shift strategy in the infection phase to impove the virus productivity and overcome the "cell density effect."

Table 2 Comparison of cell growth and virus production in shake flasks (SFs) and bioreactor (ATF1)

	SFs	ATF1
VCC at TOI ($\times 10^6$ cells/mL)	44.4	40.8
Viability at TOI (%)	97.4	91.0
Virus titer ($\log_{10}$(HAU/100 μL))[a]	4.25	3.92
CSVY (virions/cell)[b]	7638	4077
CSPR (cell growth) (pL/cell/h)[c]	61.0	71.8
CSPR (virus production) (pL/cell/h)[d]	63.2	99.4

VCC, viable cell concentration; *TOI*, time of infection; *HAU*, hemagglutination units; *CSVY*, cell-specific virus yield; *CSPR*, cell-specific perfusion rate

[a] The accumulated titer obtained in the infection phase

[b] CSVY as defined by Eq. (6) in Section 2.5

[c] The average CSPR based on measurements from the time of inoculation to the time of infection

[d] The averagel CSPR based on measurements from the time of infection to the end of cultivation

Optimized ATF perfusion process: manual versus automated perfusion control

As a final step towards process optimization, two additional bioreactor runs (ATF4 and ATF5) were carried out with a lower CSPR and on-line perfusion control (Table 1). Compared to the CSPR of 60 pL/cells/day used in previous runs, a CSPR of 40 pL/cell/day was used in ATF4 and ATF5 runs to reduce the medium consumption. Furthermore, a capacitance probe was used in the ATF5 run for on-line monitoring of the viable cell concentration for perfusion rate control. With this set-up, no manual adjustments of the perfusion pump were necessary.

For on-line monitoring, we correlated the on-line permittivity signal with off-line cell counts (ATF5). As already seen for other cultivations at HCD using a capacitance probe (Nikolay et al. 2018; Vazquez-Ramirez et al. 2019), the permittivity signal correlated well ($R^2 > 99\%$) to the off-line viable cell concentration measurements during the cell growth phase in HCD ($> 40 \times 10^6$ cells/mL)

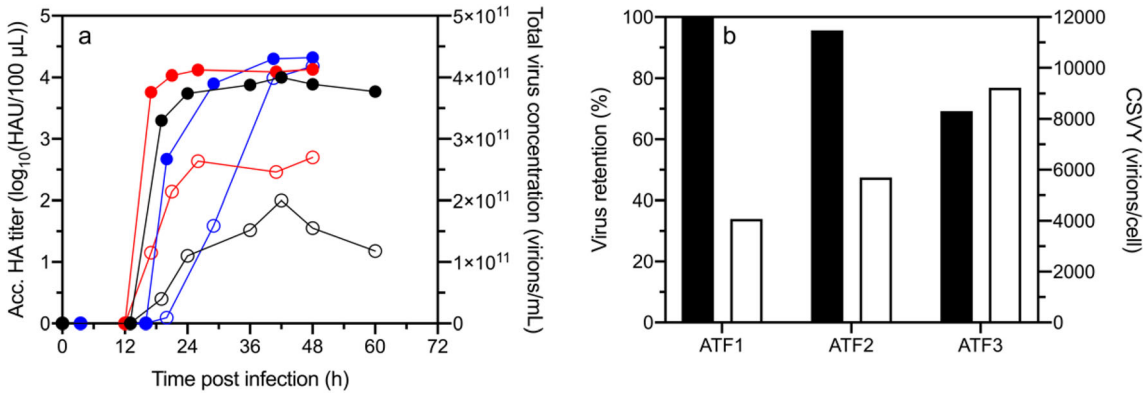

Fig. 3 Virus production of ATF1–3 using MDCK suspension cells at high cell density. (a) Accumulated HA titer (solid circle) and total virus concentration (open circle). (b) Virus retention (the ratio of virus particles in the bioreactor to the total virus particles) by ATF membrane (black columns) and cell-specific virus yield (white columns). ATF1 (●), ATF2 (●), ATF3 (●)

despite changes in the cell diameter (Fig. 4a). Thereby, the perfusion rate could be controlled with the defined CSPR in the cell growth phase. Similar cell factors for the cell growth phase were obtained from other runs (data not shown), which demonstrated the comparability between bioreactor runs. However, after the trypsin addition at TOI, a decline in the permittivity signal was observed and the corresponding on-line viable cell concentration value was "recovering" to the actual value (off-line cell count) only after approximately 12 h (Fig. 4c). Furthermore, in the late infection phase, the background noise of ViCell images was increased and measurements were biased due to the increase of cell debris in the culture. All these led to a change of the cell factor to 0.50 ($R^2 = 0.80$) in the infection phase compared to the cell growth phase (cell factor = 0.91) (Fig. 4b).

The reduction of the CSPR to 40 pL/cell/day in both runs enabled a high cell concentration to approximately 40×10^6 cells/mL with an increase of doubling time from 17 to 46 h during the growth phase, which overall was comparable to the CSPR 60 pL/cell/day runs (Fig. 5a). Cell diameters were slowly decreasing from 15.3 to 13.4 µm during the perfusion before infection despite a decrease in osmolality in both runs (Fig. 5b). Based on the higher buffer capacity of Xeno-CDM2 and a reduction in base addition to control pH values, the formation of cell aggregates in the cell growth phase was largely avoided. After infection, high virus titers (30–35% of the virus concentration in the bioreactors) were measured in the harvest for both runs. Accordingly, similar accumulated virus yields were obtained with the ATF4 run ($HA_{acc} = 4.42$ $\log_{10}(HAU/100\ \mu L)$, $C_{tot} = 5.3 \times 10^{11}$ virions/mL, $TCID_{50,acc} = 1.8 \times 10^{10}$ virions/mL) compared to the ATF5

Table. 3 Comparison of MDCK cell–based IAV production for batch cultivations in STR and ATF-based perfusion cultivations in STR

	Max. cell concentration	Accumulated HA	Total virus concentration	Total infectious virus concenntration	CSVY	STVY	Vol. productivity
	10^6 cells/mL [a]	Log_{10}(HAU/100 µL)[b]	10^{11} virions/mL[c]	10^9 virions/mL[d]	virions/cell	10^{13} virions/L/day[e]	10^{13} virions/L/day[f]
Batch	7.6	3.60	0.8	2.7	10,476	1.6	1.93
ATF1	40.8	3.92	1.7	18	4077	2.1	0.20
ATF2	46.3	4.12	2.6	n.d.	5694	3.8	0.37
ATF3	50.8	4.37	4.7	15	9229	7.1	0.55
ATF4	45.0	4.42	5.3	18	11,690	8.0	1.02
ATF5	43.3	4.37	4.7	20	10,827	7.4	1.00

HA, hemagglutinin; *TCID*$_{50}$, 50% tissue culture infective dose; *CSVY*, cell-specific virus yield; *STVY*, space time virus yield

[a] In the infection phase

[b] Accumulated HA of each run

[c] Total virus concentration of each run; calculated with Eq. (5) in Section 2.5

[d] Total infectious virus concentration of each run; calculated with Eq. (4) in Section 2.5

[e] STVY was calculated based on Eq. (7) shown in Section 2.5

[f] Vol. productivity was calculated based on Eq. (8) shown in Section 2.5

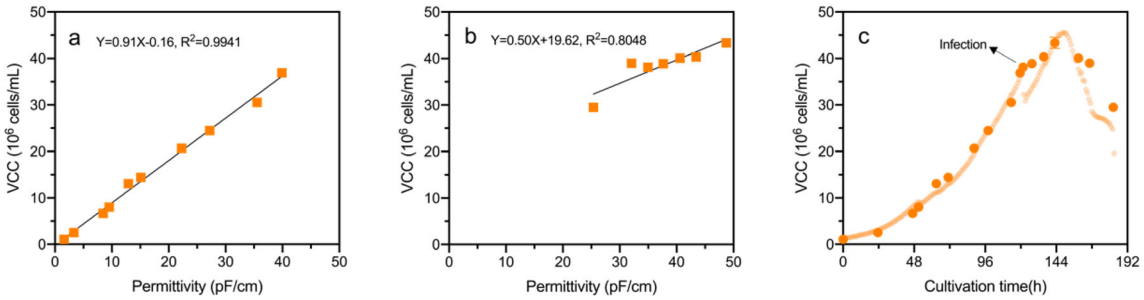

Fig. 4 Use of a capacitance probe for monitoring viable cell concentration (VCC) of a ATF bioreactor perfusion process for IAV production (ATF5). Correlation of the off-line measured VCC to the on-line monitored permittivity signal for (a) the cell growth phase and (b) the virus infection phase. The slope of the regression line corresponded to a cell factor of 0.91 in the cell growth phase and 0.50 in the infection phase. (c) Comparison of the estimated VCC (●) and the off-line measured cell count (●). Off-line measurements represent the mean of duplicate measurements. Arrow indicates the time of infection

run ($HA_{acc} = 4.37$ $\log_{10}$(HAU/100 μL), $C_{tot} = 4.7 \times 10^{11}$ virions/mL, $TCID_{50,acc} = 2.0 \times 10^{10}$ virions/mL) (Fig. 5c and d and Table 3).

The manual adjustment of perfusion rates (ATF1-ATF4) between the samplings resulted in a temporary overfeeding and may have affected cell growth. The use of the capacitance probe for perfusion rate control could result in a more stable metabolic state as well as in a decrease in the volume of perfusion medium (Fig. 6). Indeed, due to more precise perfusion rate control, a lower volume of perfusion medium (3.88 L, 7.8 RV) was required in the ATF5 run compared to the ATF4 run (4.42 L, 8.8 RV) (Fig. 7a). Correspondingly, compared to the ATF3 run with a higher CSPR, 32% (ATF5) and 23% (ATF4) of the medium were saved. Overall, the ATF5 run represents a 5-fold increase in volumetric virus productivity than the initial ATF1 run. Clearly, on-line biomass measurements enabled a better control of the perfusion rate at the defined 40 pL/cell/day for the ATF5 run (Fig. 7b).

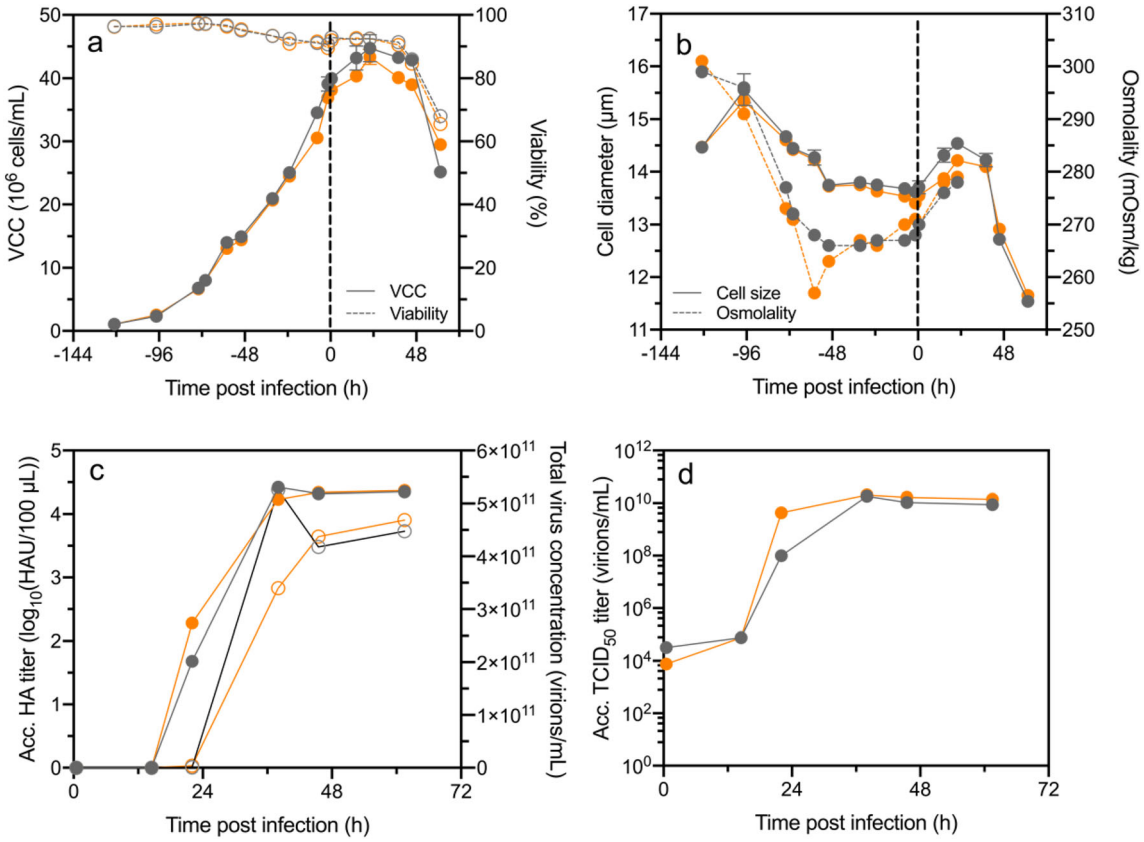

Fig. 5 Cell growth and virus titers of the optimized perfusion processes ATF4 and ATF5 for IAV production. (a) Viable cell concentration and viability, (b) cell diameter (solid line) and culture osmolality (dashed line), (c) accumulated HA titer (solid circle) and total virus concentration (open circle), and (d) accumulated $TCID_{50}$ titer. ATF4 (●), ATF5 (●). Vertical dashed lines indicate time of infection. The error bars represent the standard deviation of duplicate measurements

Similar metabolic profiles for the main extracellular metabolites and amino acids were obtained in both runs. During the cell growth phase using a CSPR of 40 pL/cell/day, main metabolite concentrations slightly decreased but showed no limitation (glucose > 15 mM, glutamine > 1 mM) before infection. Stable profiles and no obvious limitations of measured amino acids were also observed for the cell growth phase, with the exception of isoleucine, methionine, and leucine (Fig. 6). The concentrations of these three amino acids were below the limit of quantification (0.25 mM) of HPLC method. A partial medium exchange was conducted by increasing the perfusion rate for 2 h in both runs at 121 h before infection to avoid potential substrate limitation and inhibitor accumulation. This resulted in an increase in the concentrations of glucose, glutamine, and amino acids, and a decrease of lactate and ammonium at TOI. Nevertheless, in the infection phase, a steep decrease in glucose concentration (< 5 mM) and a significant accumulation of lactate concentration (> 45 mM) were observed (Fig. 6b). A similar pattern was not found, however, at the same stage for the ATF3 run with a CSPR of 60 pL/cell/day (Fig. S2). Thus, during the infection phase (22–34 hpi), it was decided to do a CSPR adjustment for sufficient supply of metabolites in the infection phase. The situation was improved by a temporary manual operation of increasing CSPR to 60 pL/cell/day for 12 h. As a result, the glucose limitation was resolved and the lactate concentration was reduced (Fig. 6a and b). Ammonium, a critical factor for virus yield, was maintained at around 3 mM in the infection phase, which is a common concentration reported in literature (Fig. 6c and d) (Glacken et al. 1986; Coronel et al. 2019). Therefore, no inhibition of viral replication was expected.

Discussion

For timely manufacturing of influenza vaccines guarantieeing a sufficient supply, particularly in the case of a pandemic outbreak, process intensification by means of high cell density cultivation has several advantages. First, it significantly improves virus yields. Second, based on a suitable cell line with high growth and production performance, production capacity can be enhanced. Thus, in this work, we developed an efficient and competitive ATF-based perfusion process using a previously developed MDCK suspension cell line that grows in CDM for IAV production.

Concentrations over 40×10^6 viable cells/mL were achieved in small-scale experiments using SFs with a CSPR-based strategy. With a further increase in medium exchange steps, higher cell

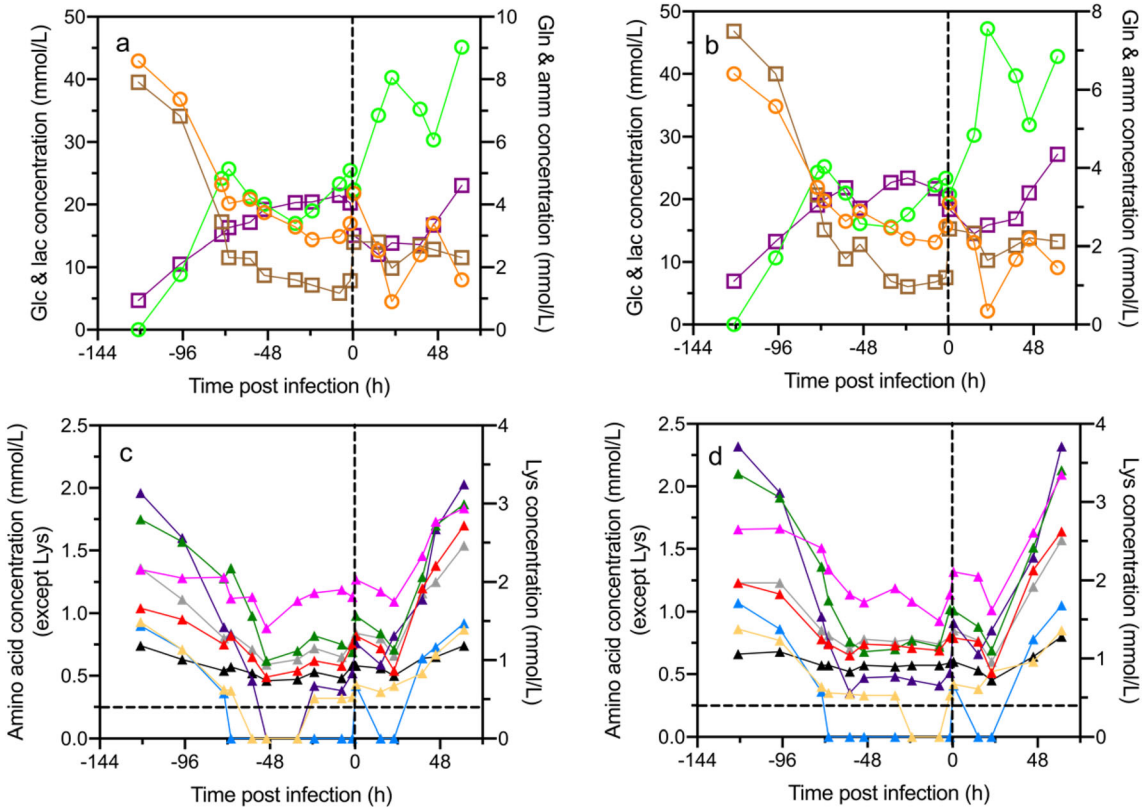

Fig. 6 Extracellular metabolites of the optimized perfusion processes ATF4 and ATF5 for IAV production. (a) Glucose (◯), glutamine (□), lactate (◯), and ammonium (□) concentration of (a) ATF4 and (b) ATF5; amino acids (threonine (▲), lysine (▲), methionine (▲), valine (▲), isoleucine (▲), leucine (▲), phenylalanine (▲), tryptophan (▲)) concentration of (c) ATF4 and (d) ATF5. Vertical dashed lines indicate time of infection. Horizontal dashed lines indicate the limit of detection for amino acids

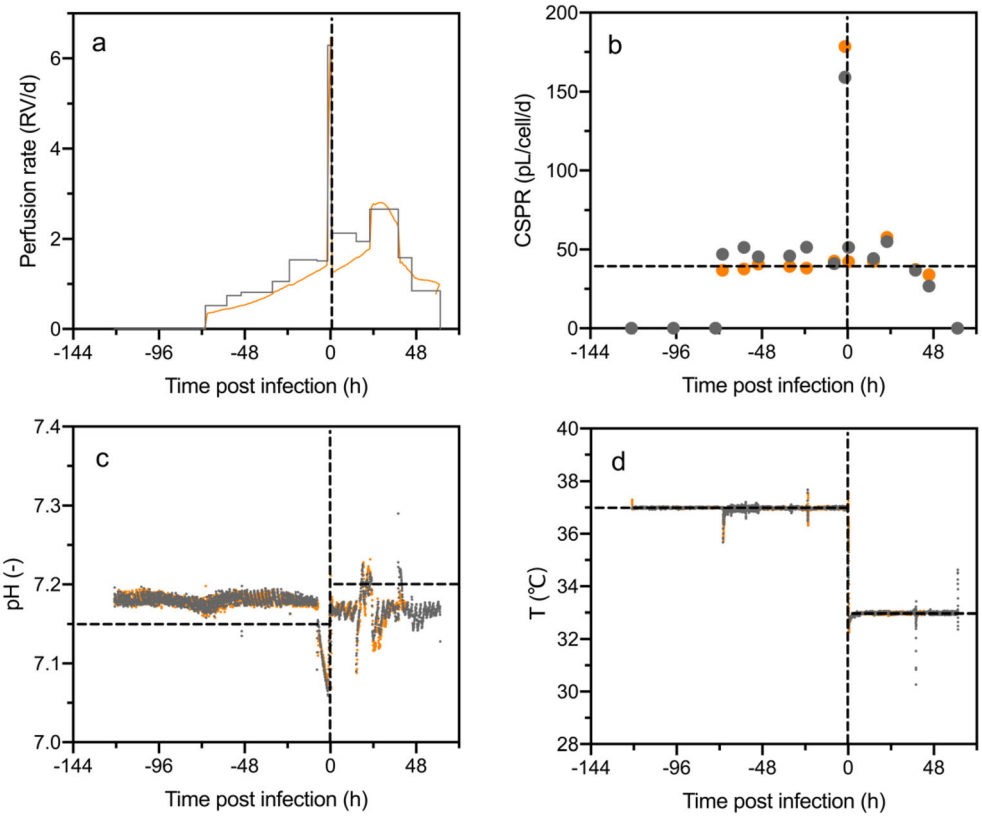

Fig. 7 Process parameters of the optimized perfusion processes ATF4 and ATF5 for IAV production. (a) Perfusion rate, (b) cell-specific perfusion rate, (c) pH value, (d) temperature (ATF4 (▲), ATF5 (●). Vertical dashed lines indicate time of infection. Horizontal dashed lines indicate set points of process parameters for both runs

concentrations might be possible but this may lead to process instability (lower specific growth rate, cell damage, and loss). In addition, manual medium exchanges are limited to time intervals that still allow for centrifugation and medium renewal (Bissinger et al. 2019). As one of the critical factors for virus infection at HCD, the MOI needs to be selected carefully (Merten et al. 1999; Wang et al. 2017). In preliminary scale-down experiments (MOI 0.1 vs. 0.001, data not shown) comparable virus titers were obtained. Considering that it can be advantageous to shorten preparation time for the seed virus stock in large-scale production and to reduce the risk of accumulation of defective interfering particles, the lower MOI was used here (Isken et al. 2012; Youil et al. 2004). This HCD process with a HA titer of 4.25 $\log_{10}$(HAU/100 μL) in SFs clearly outperformed MDCK-based IAV production processes described before, and showed one of the highest HA titers ever reported (Chu et al. 2009; Huang et al. 2015; Peschel et al. 2013; Tapia et al. 2014; Wang et al. 2017).

Regarding the temperature shift, the suppression of cell growth at reduced temperature appears to be a well-known phenomenon in antibody and some other virus production processes; and its impact was thus confirmed again for IAV production at HCD in this work (Andersen et al. 2000; Jardon and Garnier 2003; Yoon et al. 2005). The reduction of temperature in the infection phase (ATF3–5) improved virus titers (HA titer over 4.37 $\log_{10}$(HAU/100 μL)) compared to the initial bioreactor runs. Lower level of extracellular toxic by-products lactate and ammonia during the infection phase can be one possible explanation for the higher overall virus yield in the temperature shift run (Fig. S2). In addition, continuous removal of virus particles via the ATF membrane most likely also reduced the unspecific virion degradation by enzymes released from lysing cells in the bioreactor. Finally, a reduction of the temperature may also affect the antigenic conformation of HA epitopes and therefore have an impact on vaccine quality as reported before for dengue virus (Boigard et al. 2018). Clearly, further investigations on IAV antigenicity and immunogenicity in animal models should be performed to support this hypothesis.

An ATF membrane of 0.2 μm cut-off was used for cell retention in this work and has been also applied successfully for other processes including yellow fever virus and Zika virus production (Nikolay et al. 2018). IAV particles have a mean diameter of only about 100 nm and should theoretically be able to pass 0.2-μm pore size membranes. However, HA titer in the harvest in ATF1 and ATF2 runs was very low, which was consistent with results reported previously (Genzel et al. 2014). Surprisingly, with the temperature shift to 33 °C during virus production, about half of the virus particles released (45%) crossed the membrane and were collected in the harvest vessel. Despite the observed lower virus retention using lower process temperature, membrane fouling was observed during the virus production phase which decreased membrane permeability over time (Fig. S1). This needs further investigation regarding the contaminant (host DNA and protein) levels and membrane fouling in the cultivations.

The use of a capacitance probe for viable cell monitoring allowed to control the perfusion rate and therefore contributed significantly to establish the ATF-based stragegy in bioreactors. However, trypsin addition at TOI resulted in a decrease in permittivity signal and interfered with measurements. This was also described previously in a HEK293 cell–based IAV production process but with a temporary increase in permittivity (Petiot et al. 2017). In the early infection phase of our cultivations, the lower VCC estimated resulted in a reduction of the perfusion rate, which might have been one of the reasons for the temporary substrate limitation (e.g., glucose) in the ATF5 run (Fig. 6b). Overall, the adaptation of the on-line CSPR control is necessary for the infection phase due to the alteration of the cell factor and to provide enough substrates for virus replication.

Overall, an optimized and fully automatized perfusion process was established with a capacitance sensor-based process control, high virus yields (HA titer: over 4.37 $\log_{10}$(HAU/100 μL), $TCID_{50}$ titer: 2.0×10^{10} virions/mL) and high process economy. High virus yields can be attributed to the combination of the high cell concentration during the infection phase, the high CSVY obtained after process optimization, and the reduction of unspecific virus degradation via continuous permeate removal. To our knowledge, the presented process is the first scalable ATF-based perfusion process for cultivation of MDCK suspension cells in CDM. Furthermore, the obtained virus titers are the highest reported for bioreactor processes both for MDCK cells and other cell lines, so far (Coronel et al. 2019; Genzel et al. 2014; Granicher et al. 2019; Vazquez-Ramirez et al. 2019). Additionally, the CSVY was comparable and the STVY was about 5-fold higher than for the established conventional batch process (Table 3), which clearly demonstrates the high process performance of intensified HCD processes for H1N1 virus production. Further process improvements could focus on medium optimization with respect to potential limiting amino acids or a designed feed medium for virus production to allow for a more efficient substrate utilization (Aucoin et al. 2007; Xie et al. 2019). Additionally, other human IAV A and B strains could be tested with this platform for the potential manufacturing of polyvalent vaccine candidates. Clearly, in line with current needs to develop new vaccines for emerging diseases very fast, our approach could serve as a model for the development of intensified platform processes in the cell culture–based vaccine manufacturing.

Supplementary Information The online version contains supplementary material available at https://doi.org/10.1007/s00253-020-11050-8.

Acknowledgments The authors would like to thank Claudia Best, Nancy Wynerski, Susanna Koenig, and Heike Sperlich for their excellent technical assistance in terms of general lab work and virus sample analysis.

Author contributions YW, TB, YG, XL, UR, and W-ST conceived and designed the study. YW performed the experiments. YW, TB, YG, and XL analyzed the data. YW wrote the manuscript. All authors read, revised, and approved the manuscript.

Funding Yixiao Wu acknowledges the financial support from the China Scholarship Council.

Data availability The datasets generated during and/or analyzed during the current study are available from the corresponding author on reasonable request.

Compliance with ethical standards

Conflict of interest Wen-Song Tan and Xuping Liu are affiliated as directors with Shanghai BioEngine Sci-Tech and were involved in the development of the Xeno-CDM medium both for scientific and commercial purposes. The remaining authors declare that they have no conflict of interest.

Ethics approval This article does not contain any studies with human participants or animals performed by any of the authors.

Consent to participate Not applicable

Consent for publication Not applicable

Code availability Not applicable

References

Andersen DC, Bridges T, Gawlitzek M, Hoy C (2000) Multiple cell culture factors can affect the glycosylation of asn-184 in CHO-produced tissue-type plasminogen activator. Biotechnol Bioeng 70(1):25–31

Ansorge S, Esteban G, Schmid G (2007) On-line monitoring of infected Sf-9 insect cell cultures by scanning permittivity measurements and comparison with off-line biovolume measurements. Cytotechnology 55(2–3):115–124. https://doi.org/10.1007/s10616-007-9093-0

Aucoin MG, Perrier M, Kamen AA (2007) Improving AAV vector yield in insect cells by modulating the temperature after infection. Biotechnol Bioeng 97(6):1501–1509. https://doi.org/10.1002/bit.21364

Bissinger T, Fritsch J, Mihut A, Wu Y, Liu X, Genzel Y, Tan W-S, Reichl U (2019) Semi-perfusion cultures of suspension MDCK cells enable high cell concentrations and efficient influenza A virus production. Vaccine 37(47):7003–7010. https://doi.org/10.1016/j.vaccine.2019.04.054

Boigard H, Cimica V, Galarza JM (2018) Dengue-2 virus-like particle (VLP) based vaccine elicits the highest titers of neutralizing antibodies when produced at reduced temperature. Vaccine 36(50):7728–7736. https://doi.org/10.1016/j.vaccine.2018.10.072

Carvell JP, Dowd JE (2006) On-line measurements and control of viable cell density in cell culture manufacturing processes using radio-frequency impedance. Cytotechnology 50(1–3):35–48. https://doi.org/10.1007/s10616-005-3974-x

Chu C, Lugovtsev V, Golding H, Betenbaugh M, Shiloach J (2009) Conversion of MDCK cell line to suspension culture by transfecting with human siat7e gene and its application for influenza virus production. PNAS 106(35):14802–14807 www.pnas. https://doi.org/10.1073/pnas.0905912106

Coronel J, Behrendt I, Burgin T, Anderlei T, Sandig V, Reichl U, Genzel Y (2019) Influenza A virus production in a single-use orbital shaken bioreactor with ATF or TFF perfusion systems. Vaccine 37(47):7011–7018. https://doi.org/10.1016/j.vaccine.2019.06.005

Emma P, Kamen A (2013) Real-time monitoring of influenza virus production kinetics in HEK293 cell cultures. Biotechnol Prog 29(1): 275–284. https://doi.org/10.1002/btpr.1601

Fauci AS (2006) Seasonal and pandemic influenza preparedness: science and countermeasures. J Infect Dis 194:S73–S76

Genzel Y, Reichl U (2007) Vaccine Production. In: Vaccine production animal cell biotechnology: methods and protocols, 2rd edn. Humana Press, Totowa, pp 457–473

Genzel Y, Reichl U (2009) Continuous cell lines as a production system for influenza vaccines. Expert Rev Vaccines 8(12):1681–1692

Genzel Y, Vogel T, Buck J, Behrendt I, Ramirez DV, Schiedner G, Jordan I, Reichl U (2014) High cell density cultivations by alternating tangential flow (ATF) perfusion for influenza A virus production using suspension cells. Vaccine 32(24):2770–2781. https://doi.org/10.1016/j.vaccine.2014.02.016

Glacken M, Fleischaker R, Sinskey A (1986) Reduction of waste product excretion via nutrient control: possible strategies for maximizing product and cell yields on serum in cultures of mammalian cells. Biotechnol Bioeng 28:1376–1389. https://doi.org/10.1002/bit.260280912

Granicher G, Coronel J, Pralow A, Marichal-Gallardo P, Wolff M, Rapp E, Karlas A, Sandig V, Genzel Y, Reichl U (2019) Efficient influenza A virus production in high cell density using the novel porcine suspension cell line PBG.PK2.1. Vaccine 37(47):7019–7028. https://doi.org/10.1016/j.vaccine.2019.04.030

Henry O, Dormond E, Perrier M, Kamen A (2004) Insights into adenoviral vector production kinetics in acoustic filter-based perfusion cultures. Biotechnol Bioeng 86(7):765–774

Hoffmann M, Kleine-Weber H, Schroeder S, Krüger N, Herrler T, Erichsen S, Schiergens TS, Herrler G, Wu N-H, Nitsche A, Müller MA, Drosten C, Pöhlmann S (2020) SARS-CoV-2 cell entry depends on ACE2 and TMPRSS2 and is blocked by a clinically proven protease inhibitor. Cell 181(2):271-280.e8 https://doi.org/10.1016/j.cell.2020.02.052

Hu AY, Tseng YF, Weng TC, Liao CC, Wu J, Chou AH, Chao HJ, Gu A, Chen J, Lin SC, Hsiao CH, Wu SC, Chong P (2011) Production of inactivated influenza H5N1 vaccines from MDCK cells in serum-free medium. PLoS One 6(1):e14578. https://doi.org/10.1371/journal.pone.0014578

Huang D, Peng WJ, Ye Q, Liu XP, Zhao L, Fan L, Xia-Hou K, Jia HJ, Luo J, Zhou LT, Li BB, Wang SL, Xu WT, Chen Z, Tan WS (2015) Serum-free suspension culture of MDCK cells for production of influenza H1N1 vaccines. PLoS One 10(11):e0141686. https://doi.org/10.1371/journal.pone.0141686

Isken B, Genzel Y, Reichl U (2012) Productivity, apoptosis, and infection dynamics of influenza A/PR/8 strains and A/PR/8-based reassortants. Vaccine 30(35):5253–5261. https://doi.org/10.1016/j.vaccine.2012.05.065

Jardon M, Garnier A (2003) pH, pCO2 temperature effect on R-adenovirus production. Biotechnol Prog 19:202–208

Jia X, Li Y, Fan W, Sun Q, Zhou T, Lin W, Li J (2016) Effects of temperature and pH on the growth of H1N1 subtype of influenza A virus by surface-enhanced Raman spectroscopy. Sheng Wu Gong Cheng Xue Bao 32(4):447-456 https://doi.org/10.13345/j.cjb.150362

Kalbfuss B, Knöchlein A, Kröber T, Reichl U (2008) Monitoring influenza virus content in vaccine production: precise assays for the quantitation of hemagglutination and neuraminidase activity. Biologicals 36(3):145–161. https://doi.org/10.1016/j.biologicals.2007.10.002

Kiss B, Németh Á (2016) Application of a high cell density capacitance sensor to different microorganisms. Period Polytech-Chem 60(4): 290–297. https://doi.org/10.3311/PPch.8824

Kistner O, Barrett P, Mundt W, Reiter M, Schober-Bendixen S, Eder G, Dorner F (1999) Development of a Vero cell-derived influenza whole virus vaccine. Dev Biol Stand 98:101–110

Konstantinov K, Goudar C, Ng M, Meneses R, Thrift J, Chuppa S, Matanguihan C, Michaels J, Naveh D (2006) The "push-to-low" approach for optimization of high-density perfusion cultures of animal cells cell culture engineering. Adv Biochem Engin/Biotechnol, pp:75–98

Lambert LC, Fauci AS (2010) Influenza vaccines for the future. New Engl J Med 363:2036–2044. https://doi.org/10.1056/NEJMra1002842

Maranga L, Brazao TF, Carrondo MJ (2003) Virus-like particle production at low multiplicities of infection with the baculovirus insect cell system. Biotechnol Bioeng 84(2):245–253. https://doi.org/10.1002/bit.10773

McLean KA, Goldin S, Nannei C, Sparrow E, Torelli G (2016) The 2015 global production capacity of seasonal and pandemic influenza vaccine. Vaccine 34(45):5410–5413. https://doi.org/10.1016/j.vaccine.2016.08.019

Merten OW, Manuguerra JC, Hannoun C, van der Werf S (1999) Production of influenza virus in serum-free mammalian cell cultures. Dev Biol Stand 98:23–37

Nakamura K, Harada Y, Takahashi H, Trusheim H, Bernhard R, Hamamoto I, Hirata-Saito A, Ogane T, Mizuta K, Konomi N, Konomi Y, Asanuma H, Odagiri T, Tashiro M, Yamamoto N (2019) Systematic evaluation of suspension MDCK cells, adherent MDCK cells, and LLC-MK2 cells for preparing influenza vaccine seed virus. Vaccine 37(43):6526–6534. https://doi.org/10.1016/j.vaccine.2019.08.064

Nikolay A, Leon A, Schwamborn K, Genzel Y, Reichl U (2018) Process intensification of EB66 cell cultivations leads to high-yield yellow fever and Zika virus production. Appl Microbiol Biotechnol 102(20):8725–8737. https://doi.org/10.1007/s00253-018-9275-z

Peschel B, Frentzel S, Laske T, Genzel Y, Reichl U (2013) Comparison of influenza virus yields and apoptosis-induction in an adherent and a suspension MDCK cell line. Vaccine 31(48):5693–5699. https://doi.org/10.1016/j.vaccine.2013.09.051

Petiot E, Ansorge S, Rosa-Calatrava M, Kamen A (2017) Critical phases of viral production processes monitored by capacitance. J Biotechnol 242:19–29. https://doi.org/10.1016/j.jbiotec.2016.11.010

Rodriguez J, Spearman M, Tharmalingam T, Sunley K, Lodewyks C, Huzel N, Butler M (2010) High productivity of human recombinant beta-interferon from a low-temperature perfusion culture. J Biotechnol 150(4):509–518. https://doi.org/10.1016/j.jbiotec.2010.09.959

Sandberg H, Lutkemeyer D, Kuprin S, Wrangel M, Almstedt A, Persson P, Ek V, Mikaelsson M (2006) Mapping and partial characterization of proteases expressed by a CHO production cell line. Biotechnol Bioeng 95(5):961–971. https://doi.org/10.1002/bit.21057

Sun K, Ye J, Perez DR, Metzger DW (2011) Seasonal FluMist vaccination induces cross-reactive T cell immunity against H1N1 (2009) influenza and secondary bacterial infections. J Immunol 186(2): 987–993. https://doi.org/10.4049/jimmunol.1002664

Tapia F, Vogel T, Genzel Y, Behrendt I, Hirschel M, Gangemi JD, Reichl U (2014) Production of high-titer human influenza A virus with adherent and suspension MDCK cells cultured in a single-use hollow fiber bioreactor. Vaccine 32(8):1003–1011. https://doi.org/10.1016/j.vaccine.2013.11.044

Tapia F, Vazquez-Ramirez D, Genzel Y, Reichl U (2016) Bioreactors for high cell density and continuous multi-stage cultivations: options for process intensification in cell culture-based viral vaccine production. Appl Microbiol Biotechnol 100(5):2121–2132. https://doi.org/10.1007/s00253-015-7267-9

Vazquez-Ramirez D, Jordan I, Sandig V, Genzel Y, Reichl U (2019) High titer MVA and influenza A virus production using a hybrid fed-batch/perfusion strategy with an ATF system. Appl Microbiol Biotechnol 103(7):3025–3035. https://doi.org/10.1007/s00253-019-09694-2

Walther J, Godawat R, Hwang C, Abe Y, Sinclair A, Konstantinov K (2015) The business impact of an integrated continuous biomanufacturing platform for recombinant protein production. J Biotechnol 213:3–12. https://doi.org/10.1016/j.jbiotec.2015.05.010

Wang H, Guo S, Li Z, Xu X, Shao Z, Song G (2017) Suspension culture process for H9N2 avian influenza virus (strain Re-2). Arch Virol 162(10):3051–3059. https://doi.org/10.1007/s00705-017-3460-8

Xie P, Ye Q, Liu XP, Tan WS (2019) Development of maintenance medium using for influenza virus production and analysis of cellular metabolic characteristics. Biotechnol Bull 35(5):133–139

Yamayoshi S, Kawaoka Y (2019) Current and future influenza vaccines. Nat Med 25(2):212–220. https://doi.org/10.1038/s41591-018-0340-z

Yoon SK, Choi SL, Song JY, Lee GM (2005) Effect of culture pH on erythropoietin production by Chinese hamster ovary cells grown in suspension at 32.5 and 37.0 degrees C. Biotechnol Bioeng 89(3): 345–356. https://doi.org/10.1002/bit.20353

Youil R, Su Q, Toner TJ, Szymkowiak C, Kwan WS, Rubin B, Petrukhin L, Kiseleva I, Shaw AR, DiStefano D (2004) Comparative study of influenza virus replication in Vero and MDCK cell lines. J Virol Methods 120(1):23–31. https://doi.org/10.1016/j.jviromet.2004.03.011